Published by :
https://www.ijert.org/
An International Peer-Reviewed Journal

International Journal of Engineering Research & Technology (IJERT)
ISSN: 2278-0181
Vol. 14 Issue 12 , December - 2025

Multi-Objective Optimization of Blend Repairs in Compressor Blisks using a Genetic Algorithm Approach

Kushal Garikipati, Vishal Bidve, Surya Bodeddula
Design Engineering Department, Hyderabad, India

Hansraj Meena
Structural Engineering Department, Bengaluru, India,

***Abstract* - Blend repairs are commonly used to remove local surface damage in compressor blisks. The removed material changes the local stiffness and mass of the structure and can shift the natural frequencies closer to engine order excitation lines. To maintain vibration safety margins, the blend geometry must be selected so that critical eigenfrequencies remain sufficiently separated from the excitations while limiting the loss of material. This paper presents a technical framework for the multi objective optimization of blend repairs in a compressor blisk. The repair is described by a semi ellipsoidal volume with design variables for location, in plane radii, depth and orientation. For each candidate design, a finite element model of a blisk sector in Ansys is used to compute the natural frequencies and the mass. Two objectives are considered, one measuring how far the structural frequencies are from prescribed excitation frequencies and one measuring the removed mass. The Non-dominated Sorting Genetic Algorithm (NSGA) II is applied to generate an approximation of the Pareto front. The results show a clear tradeoff between frequency tuning and mass loss and identify repair shapes that provide improved frequency separation with acceptable material removal.**

Keywords - compressor blisk, blend repair, semi-ellipsoid, eigenfrequencies, multi-objective optimization, NSGA-II, finite-element analysis.

I. INTRODUCTION

Integrally bladed rotors (blisks) are widely used in modern compressor stages for reasons of weight reduction and aerodynamic performance. However, their unitary construction renders their replacement expensive, so local repair of surface damage is highly desirable. Defects such as foreign-object damage (FOD), erosion or fretting marks are typically removed through blend repairs, in which a small volume of material is ground away and the surface is smoothened [1].

Although the geometric extent of a blend is small, the removal of material modifies the stiffness and mass distribution of the affected blade and, through the disk coupling, of the entire blisk. Consequently, the eigenfrequencies and mode shapes may change. In the presence of periodic aerodynamic forcing and engine-order excitations, small shifts in eigenfrequencies can lead to decreased separation from excitation lines and an increased risk of high-cycle fatigue. To maintain vibration margins, the repair geometry must therefore be treated as a design variable in a constrained optimization problem.

Berger et al. proposed a multi-objective optimization of blend repairs for a compressor blisk based on an elliptical footprint and a swarm-based optimizer. Their formulation uses a frequency-tuning objective penalizing small distances between eigenfrequencies and excitation frequencies, together with the removed mass as a second objective [1].

They demonstrated that appropriately chosen repairs can substantially improve vibration behaviour relative to heuristic blends.
The present work follows the same physical rationale but extends it in two directions:

1. The repair is represented by a **three-dimensional semi-ellipsoid** on the blade surface. In addition to location, in-plane radii and orientation, the depth of the blend is treated as a design variable.
2. The optimization is performed with **NSGA-II**, a widely used multi-objective genetic algorithm, instead of PSO. NSGA-II provides intrinsic non-dominated sorting and diversity control, which is attractive when FE evaluations are expensive.

The focus of this paper is the technical formulation and implementation of this framework: parameterisation of the repair, FE model and boundary conditions, objective functions, and integration with NSGA-II.

II. PROBLEM FORMULATION

A. Geometry and Repair Parameterization

Let Ω_0 denote the structural domain of the nominal compressor blisk. A single damaged blade is represented within a cyclic-symmetry sector of the blisk. The repair is modelled as a semi-ellipsoidal volume $\Omega_b(x)$ that is removed from the blade surface, yielding the repaired domain.

$$\boldsymbol{\Omega(x) = \Omega_0 \setminus \Omega_b(x).}$$

International Journal of Engineering Research & Technology (IJERT)
ISSN: 2278-0181
Vol. 14 Issue 12 , December - 2025

A blade-fixed curvilinear coordinate system is defined on the airfoil surface. At the repair centre a local orthonormal basis $(\boldsymbol{t}_1, \boldsymbol{t}_2, \boldsymbol{n})$ is introduced, where $\boldsymbol{t}_1$ and $\boldsymbol{t}_2$ are tangential directions (approximately chordwise and spanwise, respectively) and $\boldsymbol{n}$ is the outward normal.

Any point in a neighbourhood of the repair can be written as

$$\boldsymbol{x} = \boldsymbol{c} + u\,\boldsymbol{t}_1 + v\,\boldsymbol{t}_2 + w\,\boldsymbol{n},$$

where $\mathbf{c}$ is the centre of the repair and (u, v, w) are local coordinates.

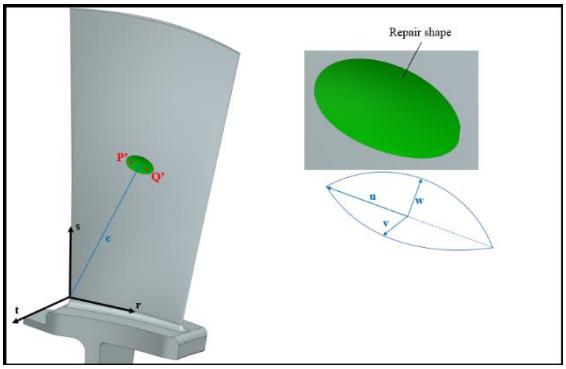

Figure 1: Geometric description of the blend repair.

The semi-ellipsoid is defined by

$$\frac{u^2}{r_u^2} + \frac{v^2}{r_v^2} + \frac{w^2}{r_w^2} \leq 1, 0 \leq w \leq r_w,$$

where r_u and r_v are the in-plane semi-axes and r_w denotes the depth of the blend. Its footprint on the airfoil is a planar ellipse with radii r_u and r_v. The in-plane orientation of this ellipse is defined by an angle θ. For convenience, a dimensionless orientation parameter $\kappa \in [-1,1]$ is used and mapped to $\theta = \kappa\,\theta_{\max}$, where $\theta_{\max}$ is a prescribed maximum rotation.

The **design vector** is

$$x = (c_r, c_s, r_u, r_v, r_w, \kappa)^{\mathrm{T}},$$

where c_r and c_s are scalar coordinates of the footprint centre in a blade-surface coordinate system – measured, for example, along a reference chordwise curve and a spanwise stacking line.

B. Design Bounds and Linear Constraints

The admissible design set $\mathcal{X}$ is defined by simple bounds and additional constraints,

$$\mathcal{X} = \{\, x \in \mathbb{R}^6 \;\mid\; x^{\mathrm{lb}} \leq x \leq x^{\mathrm{ub}},\ \mathrm{A}x \leq \mathrm{b} \,\},$$

with

$$x = [c_r \quad c_s \quad r_u \quad r_v \quad r_w \quad \kappa]^{\mathrm{T}},$$

$$x^{lb} = [10 \quad 100 \quad 10 \quad 3 \quad 0.5 \quad -1]^{\mathrm{T}}\ \mathrm{mm},$$

$$x^{ub} = [50 \quad 150 \quad 20 \quad 10 \quad 2 \quad +1]^{\mathrm{T}}\ \mathrm{mm},$$

Thus, the centre of the blend is restricted to a rectangular region on the airfoil, covering the upper mid-span zone where FOD damage is most likely to occur and where sufficient wall thickness is available.

The in-plane radii satisfy

$$r_u{}^{lb} \leq r_u \leq r_u{}^{ub}, r_v{}^{lb} \leq r_v \leq r_v{}^{ub}.$$

The minimum values are chosen slightly above $\sqrt{2}\,r_{\mathrm{mesh}}$ with a surface element size of approximately $r_{\mathrm{mesh}} = 1$ mm, following the recommendation that the footprint span several elements for robust mesh quality.

The depth is bounded by

$$0.5\ \mathrm{mm} \leq r_w \leq 2.0\ \mathrm{mm},$$

where the upper limit corresponds to the requirement that at least 60 % of the nominal wall thickness remains after repair in the studied region.

The orientation parameter is restricted to

$$-1 \leq \kappa \leq 1,$$

which is mapped to an in-plane rotation angle $\theta = \kappa\,\theta_{\max}$ with $\theta_{\max} = 45°$. Hence the major axis of the ellipse can vary within $[-45°, +45°]$ relative to the chordwise direction.

Additional constraints are introduced for crack coverage and to avoid forbidden regions, similar to the node-region constraints in Berger *et al* [1].

Crack coverage: the damaged area is idealised as a line segment with endpoints P and Q on the airfoil. Expressed in local footprint coordinates (u_P, v_P) and (u_Q, v_Q), both points must satisfy

$$\frac{u_P^2}{r_u^2} + \frac{v_P^2}{r_v^2} \leq 1, \frac{u_Q^2}{r_u^2} + \frac{v_Q^2}{r_v^2} \leq 1.$$

- Forbidden regions: a set of inequality constraints $\mathrm{A}x \leq \mathrm{b}$ ensures that the semi-ellipsoid does not intersect the platform fillet, leading edge, trailing edge or areas with insufficient thickness. Designs violating these checks are marked infeasible and assigned large objective values without running the modal analysis.

C. Modal Analysis of the Repaired Blisk Sector

For small linear vibrations, the repaired sector satisfies the semi-discrete equation of motion

$$M(x)\ddot{u}(t) + K(x)u(t) = 0,$$

where $M(x)$ and $K(x)$ denote the mass and stiffness matrices of the FE model. Assuming harmonic motion $u(t) = \phi_n(x) sin\,(\omega_n(x)t)$ leads to the generalized eigenvalue problem

$$K(x)\,\phi_n(x) = \lambda_n(x)\,M(x)\,\phi_n(x), \lambda_n(x) = \omega_n^2(x).$$

The natural frequencies are

$$\nu_n(x) = \frac{\omega_n(x)}{2\pi}, n = 1, \ldots, N,$$

with $N = 6$ in this study, consistent with the frequency range of interest reported in [1].

International Journal of Engineering Research & Technology (IJERT)
ISSN: 2278-0181
Vol. 14 Issue 12 , December - 2025

Using the same FE model, the structural mass $m(x)$ of the repaired sector is also obtained. The nominal mass m_0 corresponds to the unrepaired geometry.

D. Objective Functions

Let $\nu_{e,n}$ denote specified excitation frequencies (e.g. engine orders) associated with the considered operating point. The frequency-tuning objective is defined as

$$f_1(x) = \sum_{n=1}^{N} \frac{1}{(\nu_n(x) - \nu_{e,n})^2 + \delta^2},$$

with $\delta > 0$, a small regularization parameter representing a desired minimum frequency separation. This functional penalizes small distances $|\nu_n - \nu_{e,n}|$ and decreases when all eigenfrequencies move away from the excitations, following the concept introduced in [1].

The mass-loss objective is defined as

$$f_2(x) = \Delta m(x) = m_0 - m(x),$$

corresponding to the mass of material removed by the blend.

The multi-objective optimization problem is therefore

$$\min_{x^{lb} \le x \le x^{ub}} f(x) = \begin{bmatrix} f_1(x) \\ f_2(x) \end{bmatrix}$$

E. Pareto Optimality

For two feasible designs $x^{(a)}$ and $x^{(b)}$, $x^{(a)}$ is said to dominate $x^{(b)}$ if

$$f_i(x^{(a)}) \le f_i(x^{(b)}) (i = 1,2), \text{ and } \exists\, j: f_j(x^{(a)}) < f_j(x^{(b)}).$$

A design is Pareto-optimal if it is not dominated by any other feasible design. The set of all such designs forms the Pareto front in the objective space (f_1, f_2).

III. FINITE-ELEMENT MODEL AND COUPLING

A. Sector Model of the Compressor Blisk

The FE model represents one cyclic-symmetry sector of the compressor blisk, containing one blade and the corresponding disk segment. The geometry is imported from an NX master model into ANSYS Workbench. Tetrahedral and hexahedral solid elements are used, with local mesh refinement in the expected repair region. The reference mesh contains approximately $\mathcal{O}(10^4)$ nodes and $\mathcal{O}(10^4)$ elements.

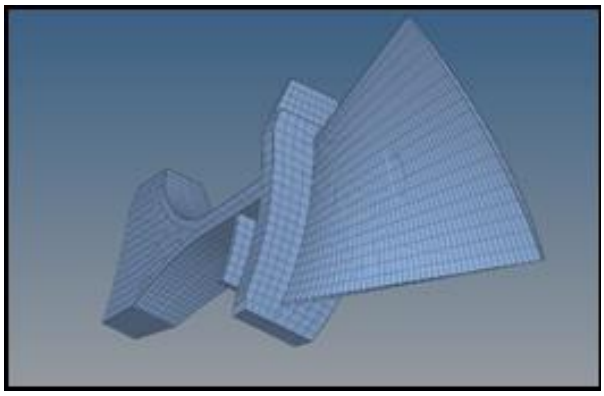

Figure 2: Node regions

Cyclic symmetry is enforced by coupling displacements at the two sector faces with appropriate phase conditions. Additional kinematic constraints are applied near the hub to suppress rigid-body motion: displacements in radial and axial directions are fixed on selected hub surfaces while tangential motion is permitted to represent rotation.

Centrifugal pre-stress is introduced by prescribing a rotational speed Ω about the rotor axis and performing a geometrically non-linear static analysis. The resulting stress state is then used as initial condition for the pre-stressed modal analysis across the operating speed range. From this analysis, the first six eigenfrequencies at the rated speed $\Omega_{\text{rated}} = 10{,}500$ rpm are extracted and used in the tuning functional $f_1(x)$. The same set of eigenfrequencies can be plotted versus rotational speed to construct a Campbell diagram, which allows one to verify the location of engine-order crossings and to identify critical resonance regions for the nominal and repaired geometries [1].

Material properties (Young's modulus, Poisson's ratio, density) correspond to the titanium alloy used in the demonstrator blisk (e.g. Ti-6Al-4V).

IV. MULTI-OBJECTIVE GENETIC ALGORITHM (NSGA-II)

A. Algorithmic Framework

The optimisation problem defined in Section II is solved using NSGA-II. NSGA-II maintains a population of candidate designs and evolves them through reproduction and selection while approximating the Pareto front. Its key mechanisms are:

- **Fast non-dominated sorting**, which assigns each individual a Pareto rank based on dominance relations.
- **Crowding-distance estimation** within each front, which measures how isolated a solution is in objective space.
- **Elitist environmental selection**, where parents and offspring are merged and the best individuals according to rank and crowding distance are retained.

B. Representation, Initialization and Parameter Settings

Each individual encodes one repair design

$$x = (c_r, c_s, r_u, r_v, r_w, \kappa).$$

The initial population is generated by Latin-hypercube sampling within the bounds. In the present study the following parameters are used:

- population size: $P = 120$ individuals,
- number of generations: $G = 60$,
- crossover probability: $p_c = 0.9$,
- mutation probability: $p_m = 0.15$.

International Journal of Engineering Research & Technology (IJERT)
ISSN: 2278-0181
Vol. 14 Issue 12 , December - 2025

This leads to a maximum of $P \times G = 7200$ FE evaluations. Due to caching of repeated parameter vectors and early rejection of infeasible designs, the effective number of full modal analyses is slightly lower (approximately 6000). This computational effort is compatible with overnight runs on a small cluster or a modern multi-core workstation.

C. Selection, Crossover and Mutation

Binary tournament selection is applied: two individuals are drawn uniformly, and the one with lower Pareto rank is selected; if both belong to the same front, the one with larger crowding distance is selected.

Recombination uses a real-coded blend crossover. For parents $\mathbf{p}_1$ and $\mathbf{p}_2$, children $\mathbf{c}_1$ and $\mathbf{c}_2$ are formed as

$$\mathbf{c}_1 = \boldsymbol{\alpha} \odot \mathbf{p}_1 + (\mathbf{1} - \boldsymbol{\alpha}) \odot \mathbf{p}_2, \mathbf{c}_2 = \boldsymbol{\alpha} \odot \mathbf{p}_2 + (\mathbf{1} - \boldsymbol{\alpha}) \odot \mathbf{p}_1,$$

where $\boldsymbol{\alpha}$ is a random vector with components uniformly distributed in $[0,1]$ and $\odot$ denotes component-wise multiplication.

Mutation is implemented by adding Gaussian perturbations to each design variable:

$$x_i^{\text{mut}} = x_i + \sigma_i \eta_i,$$

where $\eta_i \sim \mathcal{N}(0,1)$ and σ_i is chosen as a fraction of the variable range. After mutation, the design is projected back onto $[\mathbf{x}_{\text{lb}}, \mathbf{x}_{\text{ub}}]$.

D. Environmental Selection and Pareto Set Approximation

At each generation, the union of parent and offspring populations is partitioned into Pareto fronts via fast non-dominated sorting. New parents are selected by filling fronts in order of increasing rank until the population limit is reached. When the final front cannot be fully accommodated, individuals in that front are sorted by decreasing crowding distance, and those with the largest distances are retained. This procedure ensures preservation of the best-found designs (elitism) and an even spread across the front. Compared with the PSO-based archiving strategy used in [1], the NSGA-II framework provides an intrinsic approximation of the Pareto set without a separate archive [1].

V. ILLUSTRATIVE OPTIMIZATION RESULTS

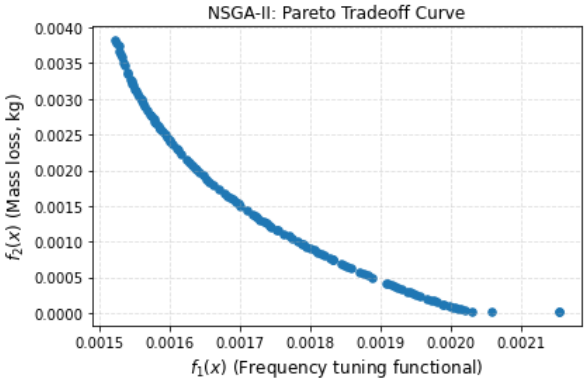

Figure 3: Pareto front illustrating the trade-offs across all eigenfrequency modes.

The algorithm was executed with a population size of P and G generations, resulting in approximately $P \times G$ FE evaluations. The computational effort is dominated by the FE modal analyses; caching and possible parallelization can significantly reduce wall-clock time.

A. Pareto Front in the (f_1,f_2) Plane

Figure 3 shows the final set of non-dominated solutions obtained by NSGA-II. Each point corresponds to a specific repair geometry. The front exhibits a typical convex shape:

- near the right-hand side, f_2 is small (little mass removed) and f_1 is relatively large (eigenfrequencies close to excitations);
- moving along the front towards lower f_1 increases the mass loss, indicating that larger and deeper blends produce more favourable tuning.

A knee region can be identified where a moderate increase in mass loss yields a substantial reduction in f_1. Designs in this region represent technically attractive compromises.

B. Eigenfrequency Deviations Versus Repaired Mass

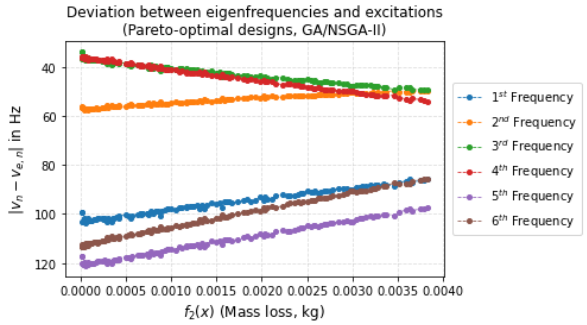

Figure 4: Eigenfrequency–excitation frequency deviations for the Pareto-optimal set.

Figure 4 presents the absolute deviations $| \nu_n(x) - \nu_{e,n} |$ for each mode n, plotted against the repaired mass $m(x) = m_0 - f_2(x)$ for the Pareto-optimal designs. Curves are obtained by ordering the Pareto set by mass and connecting points with identical mode index.

The results show which modes primarily drive the tuning objective. In typical compressor blisk applications, one bending mode and one torsional mode are found to be critical, while higher modes remain far from the excitation frequencies across the front, consistent with observations in [1].

For Pareto designs in the knee region, all absolute deviations exceed the safety band δ, indicating adequate frequency separation.

VI. CONCLUSIONS

A technical framework for the multi-objective optimization of blend repairs in compressor blisks has been presented. The approach combines:

- a semi-ellipsoidal parameterization of the repair volume with six design variables;
- two objectives reflecting frequency tuning and mass loss;

International Journal of Engineering Research & Technology (IJERT)
ISSN: 2278-0181
Vol. 14 Issue 12 , December - 2025

- a parametric sector FE model of the blisk in ANSYS Workbench; and
- the NSGA-II algorithm for multi-objective optimization.

The method yields a clear representation of the trade-off between eigenfrequency tuning and material removal through the Pareto front. Representative Pareto-optimal repairs provide improved separation between structural eigenfrequencies and excitation frequencies while limiting the loss of material. The formulation is general and can be adapted to other blisk geometries, excitation spectra and damage locations.

Future work includes the introduction of additional constraints based on stress or fatigue life, the extension to simultaneous optimization of multiple damaged blades, and the use of mode-tracking or nearest-mode strategies to further improve robustness with respect to eigenmode crossings.

REFERENCES

[1] R. Berger, J. Häfele, B. Hofmeister and R. Rolfes, “Blend Repair Shape Optimization for Damaged Compressor Blisks,” 12th World Congress on Structural and Multidisciplinary Optimization (WCSMO-12), Braunschweig, Germany, 2017.

[2] K. Deb, A. Pratap, S. Agarwal and T. Meyarivan, “A Fast and Elitist Multiobjective Genetic Algorithm: NSGA-II,” IEEE Transactions on Evolutionary Computation, vol. 6, no. 2, pp. 182–197, 2002.

[3] B. Denkena, V. Boess, D. Nespor, F. Flöter and F. Rust, “Engine Blade Regeneration: A Literature Review on Common Technologies in Terms of Machining,” International Journal of Advanced Manufacturing Technology, vol. 81, pp. 917–924, 2015.

[4] M. Bussmann and E. Bayer, “Blisk Production of the Future – Technological and Logistical Aspects of Future-Oriented Construction and Manufacturing Processes of Integrally Bladed Rotors,” 19th International Symposium on Airbreathing Engines (ISABE), Montreal, Canada, 2009.

[5] J. Kennedy and R. Eberhart, “Particle Swarm Optimization,” Proceedings of the IEEE International Conference on Neural Networks, Perth, Australia, 1995, pp. 1942–1948.

[6] Y. Shi and R. Eberhart, “A Modified Particle Swarm Optimizer,” Proc. IEEE Int. Conf. on Evolutionary Computation, Anchorage, USA, 1998, pp. 69–73.

[7] M. Young, The Technical Writer’s Handbook. Mill Valley, CA, USA: University Science Books, 1989.